ACI STRUCTURAL JOURNAL TECHNICAL PAPER

Title No. 116-S51

Undercut and Grouted Anchors as Post-Installed Shear Reinforcement

by Anthony Dondrea and Oguzhan Bayrak

Research and experience has shown that given specific loading scenarios and reinforcement configurations, reinforced concrete members may experience nonductile shear failures that can occur in sudden and brittle modes, often leading to structural collapse. It is desirable, therefore, to avoid shear failures and strengthen reinforced concrete elements with potential deficiencies. Candidates for strengthening include concrete elements that ACI 318 permits to be constructed without shear reinforcement (for example, shallow beams, joists, slabs, footings, and others) and concrete in rehabilitated or repurposed structures.

This research investigated the effectiveness of two post-installed reinforcement types (undercut anchors and grout-in-place threaded rods) for strengthening reinforced concrete beams in shear. The results from six full-scale shear tests, compared to design provisions in ACI 318-14 and AASHTO LRFD 2014, indicate that high-strength post-installed reinforcement may be used to strengthen beams in shear and achieve deformation and load capacities similar to traditionally reinforced elements.

Keywords: grout; post-installed reinforcement; retrofit; shear stiffening; undercut.

INTRODUCTION

Strengthening reinforced concrete in existing structures provides flexibility in reusing or repurposing buildings, addressing design deficiencies, and adding ductility to potentially brittle concrete members. Shear strengthening may be desirable for vulnerable members—most notably, large, lightly reinforced elements without shear reinforcement. For instance, the present ACI 318-14 building code expression for concrete shear resistance (Eq. (22.5.5.1)) is based on a lower-bound allowable shear stress in concrete developed in a 1962 ACI Report.[1] Past research, some prompted by building failures, shows the ACI shear design expression is unconservative for some member geometries. Other structures may see increased design demands due to a change in use and may require strengthening to maintain an acceptable level of safety. Also, many older concrete structures are inadequate to resist seismic forces and should be strengthened to reduce the potential for earthquake-induced failures.

The brittle nature of shear failure makes the shear strength of existing structures a major concern.

ACI Committee 364[2] identified five common methods for shear strengthening reinforced concrete members. Methods proposed by ACI Committee 364 (Fig. 1) include: 1) enlargement of the concrete section; 2) addition of internal steel or FRP reinforcement; 3) externally adhered FRP plates or strips; 4) near-surface-mounted reinforcement (NSM); and 5) addition of external reinforcement.

Recently, Kunz and Randl[3] and other researchers,[4-9] have evaluated the effectiveness of post-installed, epoxy-bonded steel bars as shear reinforcement and have shown them to be effective for improving shear strength and overall behavior. While post-installed bars chemically bonded by epoxy have received increasing amounts of research attention, less effort has been devoted to studying options that rely on discrete mechanical anchorage or reinforcement bonded by grout.

The objective of this study was to investigate the effectiveness of undercut anchors and grout-in-place threaded rods as post-installed shear reinforcement, expanding the structural retrofit knowledgebase beyond epoxy-bonded solutions.

The investigated techniques involve drilling holes in locations where shear reinforcement is desired and then either grouting steel threaded rods in place (Fig. 2(c)) or setting and tensioning undercut anchors (Fig. 2(b)). Both techniques require access to only one side of a concrete member, making them practical when access is restricted by backfill material, exterior cladding, interior finishes, or other obstacles. The effectiveness of each technique was confirmed through an experimental program conducted at The University of Texas at Austin, and retrofits were proven to produce behavior similar to elements with a comparable amount of cast-in-place transverse reinforcement.

Results of the experimental study were compared to calculations performed according to current code formulations in the United States, specifically ACI 318-14[10] (ACI 318) and the AASHTO LRFD 2014 (AASHTO) shear design provisions.[11] Despite inherent behavioral differences between traditional cast-in-place reinforcement and post-installed reinforcing bars, application of the current shear design provisions resulted in excellent estimations of the experimental capacities. On average, the ratios of tested shear strength to predicted strength for reinforced specimens were 1.05 and 0.99, respectively, based on ACI 318-14 and AASHTO LRFD, respectively. These biases are in the same range as those used in the original formulation of the LRFD methods and suggest that the predictive equations can be used directly with the code-specified resistance factors.

RESEARCH SIGNIFICANCE

Many existing reinforced concrete elements may require shear strengthening to meet demands due to deterioration,

ACI Structural Journal, V. 116, No. 3, May 2019.

MS No. S-2017-272, doi: 10.14359/51715504, received July 15, 2017, and reviewed under Institute publication policies.

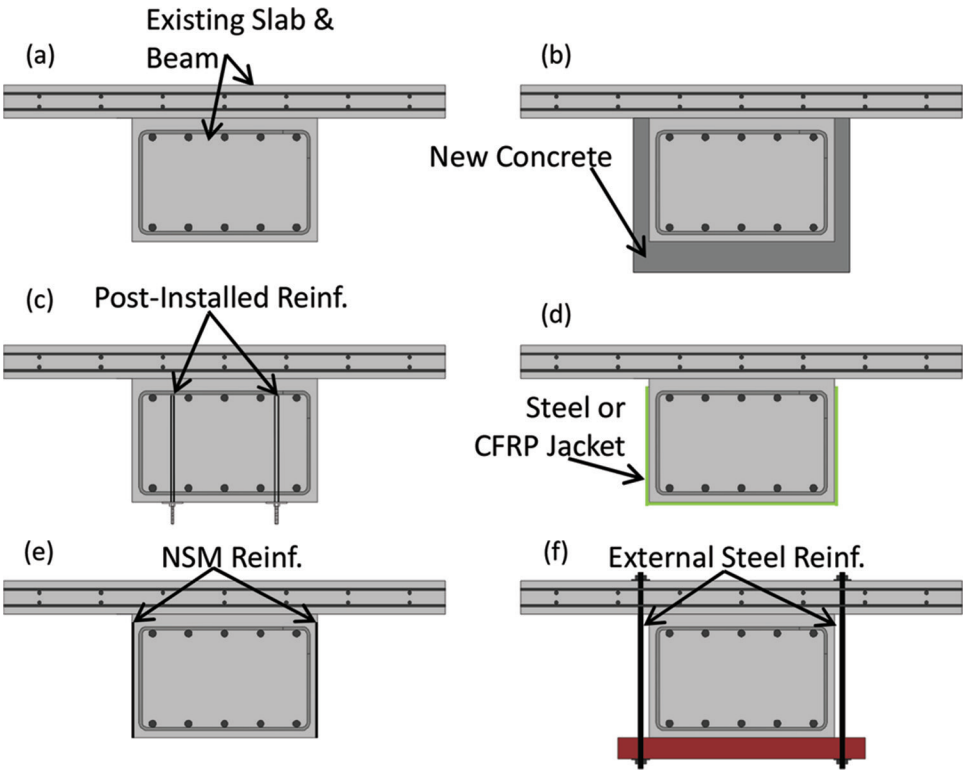

Fig. 1—Shear strengthening methods for existing RC elements: (a) unreinforced section; (b) section enlargement by additional concrete and reinforcement; (c) post-installed, bonded, or unbonded reinforcement-steel or FRP; (d) external jacketing with CFRP or steel; (e) near-surface-mounted steel or CFRP rods or bars; and (f) addition of external reinforcement.

changes in use, or other deficiencies. Other researchers[3-5] have demonstrated that post-installed chemical anchors can significantly improve the shear resistance and behavior of flat slabs and shallow beams, but research on non-epoxy anchors is limited.

This paper examines two types of post-installed steel reinforcing bars to enhance the shear strength of larger reinforced concrete members. The effectiveness of the retrofits was established through comparisons to: 1) shear tests of unreinforced and traditionally reinforced specimens; and 2) capacity estimates from the application of ACI 318-14 and AASHTO LRFD 2014.

DESCRIPTION OF RETROFIT TECHNIQUES

Figure 2 depicts the retrofit reinforcement types evaluated in this study. Throughout the paper, mechanical undercut anchors are referred to as "undercut anchors" (abbreviated as UA) and grout-in-place threaded rods as "grouted anchors" (abbreviated as GA). The undercut and grouted anchor retrofits consisted of 0.50 in. diameter (12.7 mm) high-strength threaded rods (nominal yield stress of 105 ksi [723 MPa]) installed in 0.75 in. diameter (19.0 mm) and 3.0 in.-diameter (76.2 mm) holes, respectively. All holes were diamond cored perpendicular to the longitudinal axis of the specimen and were sufficiently deep to ensure anchor embedment in the flexural compression zone of the member. Each anchor was externally anchored with a plate washer and nut on the tension face of the test specimen. After drilling, the holes were cleaned according to established best practices[12] and in agreement with recommendations by undercut anchor and grout manufacturers.

Undercut anchors were installed in accordance with the manufacturer's recommended procedures, including drilling, cleaning, and torqueing. During the torqueing process, the undercut anchor sleeve is forced over a conical nut and deforms into the undercut hole. The deformed sleeve bears against the undercut hole, allowing the anchor to resist load by mechanical interlock with the concrete.

Grouted anchors were installed in the center of a 3.0 in. diameter hole using a polycarbonate face plate centering device fitted with a valve. Grout was injected through the face plate and allowed to cure for a minimum of 5 days prior to shear testing of the specimen. Grouted anchors resist load primarily through bond at the grout-to-concrete interface.

In typical applications, post-installed anchors are subjected to a combination of axial and shear forces. The tensile and shear strengths of several kinds of post-installed anchors have been extensively studied and summarized by other researchers.[13,14] In this study, anchors installed as shear reinforcement are assumed to act in tension.

Undercut anchors in tension may fail in one or more of the following modes (depicted in Fig. 3(a), (b), and (c)): 1) yield and fracture of the undercut anchor; 2) concrete splitting between anchor locations; and 3) formation of a concrete breakout cone.[13] Headed grouted anchors in tension may fail in one or more of the following modes (depicted in Fig. 3(a), (d), and (e)): 1) yield and fracture of the rod; 2) bond failure at the grout/concrete interface; and 3) formation of a concrete breakout cone. Expressions in ACI 318-14, Chapter 17, are used to evaluate anchors' tension capacity based on the limit states previously mentioned (with the addition of grout/concrete bond failure[14]). Calculated anchor capacities were

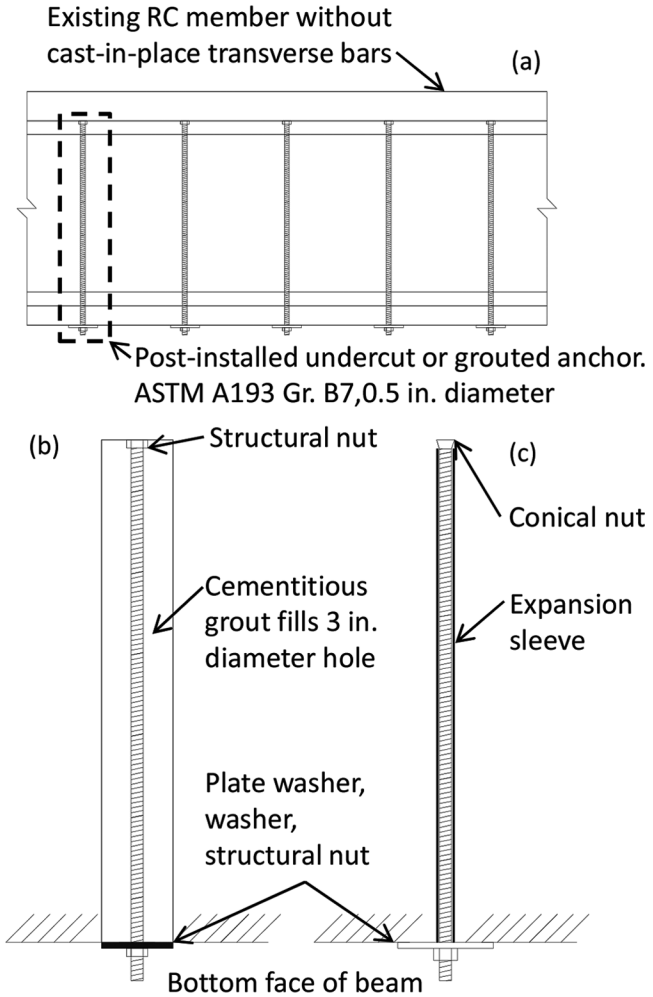

Fig. 2—Retrofit techniques under investigation: (a) schematic layout of post-installed reinforcement in a specimen without transverse reinforcement; (b) grouted anchor components; and (c) undercut anchor components.

used to predict post-installed reinforcement contribution to sectional shear strength and to develop the shear reinforcement configuration used for the experimental program.

The researchers note that undercut and grouted anchors transfer load through the concrete by different mechanisms, which may affect shear resistance (Fig. 4). For example, undercut anchors are mechanically anchored at only two points—the tension face of the member and the undercut location—and are not bonded along their length. In contrast, grouted anchors are capable of developing stress along their entire length due to bond stresses.

POST-INSTALLED ANCHOR SELECTION

Many types of bonded and mechanical post-installed anchors have proven track records in the construction industry, and this paper focuses only on two anchor types. This section briefly outlines common types of post-installed anchors and why grouted anchors and undercut anchors were selected for this study.

Common mechanical anchors include expansion- and undercut-type anchors. Expansion anchors transmit tensile loads primarily through friction between the anchor head/

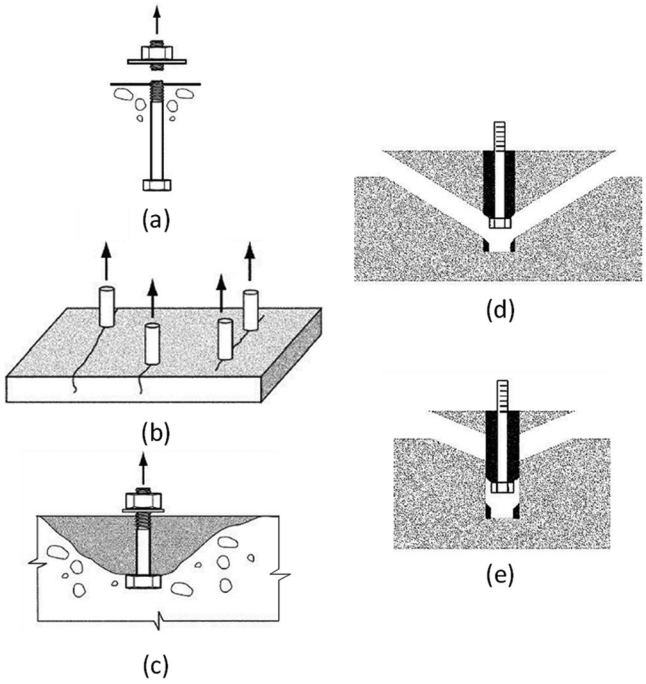

Fig. 3—Potential failure modes for post-installed anchors: (a) yield or fracture of anchor; (b) concrete splitting between anchor locations; (c) concrete breakout cone formation (undercut anchors); (d) concrete breakout cone formation (grouted anchors); and (e) bond failure at the grout/concrete interface.[10]

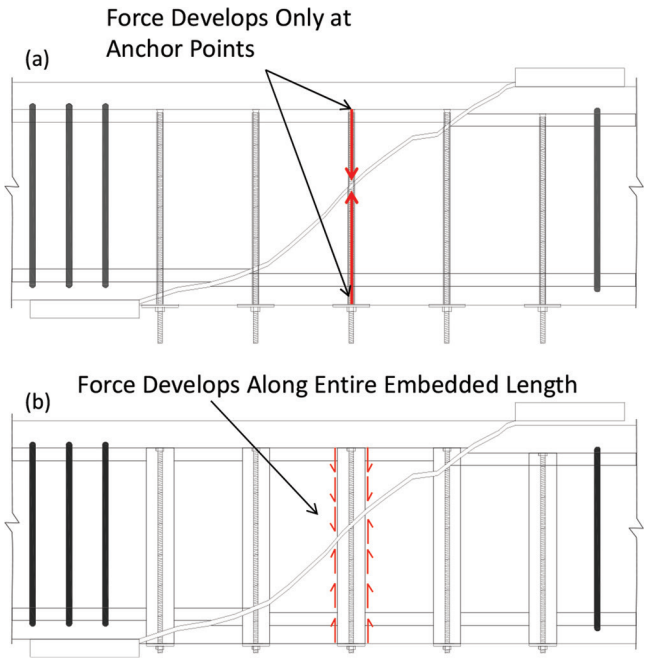

Fig. 4—Force development for post-installed reinforcement methods: (a) undercut anchors; and (b) grouted anchors. Only the test region of specimen is shown.

sleeve and the surrounding concrete. Undercut anchors transmit tensile loads through bearing between the anchor head/sleeve and the undercut concrete. Bonded anchors rely on a chemical bond between the bonding agent and the concrete substrate to resist tensile loads. Common bonding

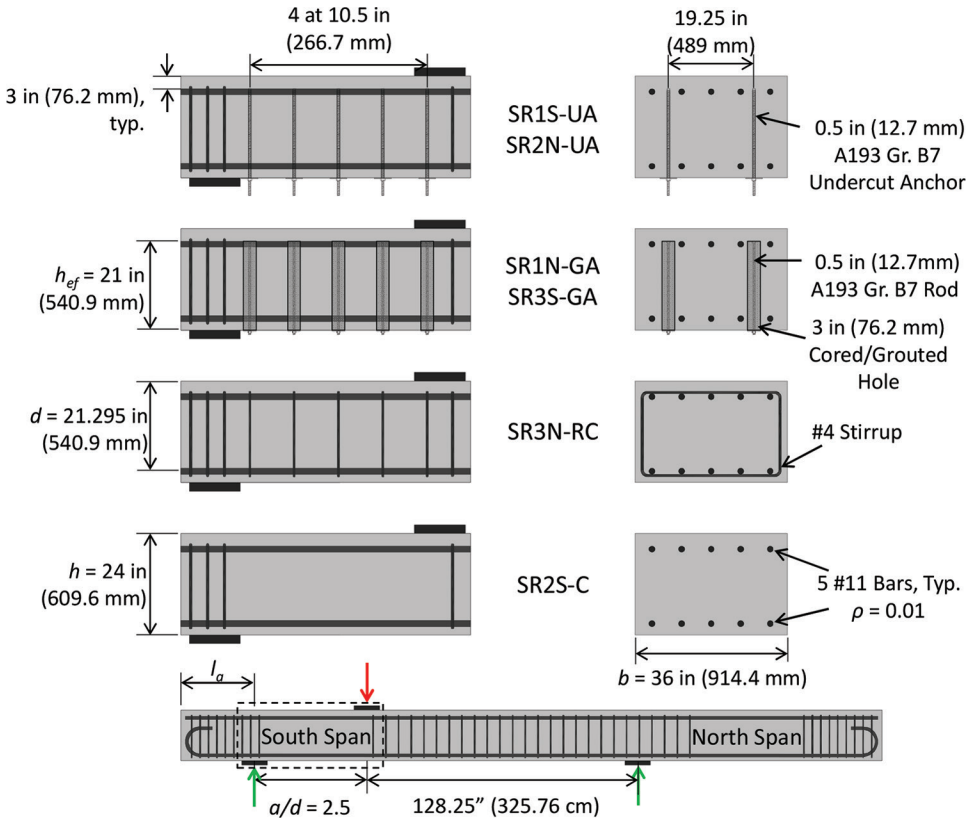

Fig. 5—Overview of test program, specimen variables, and specimen nomenclature.

agents include structural adhesives (typically epoxy) and cementitious or polymer grout.[14]

Undercut and grouted anchors were selected for this study because available research on their use as post-installed shear reinforcement is limited compared to epoxy anchors, as discussed previously. Engineers must consider many project-specific details including, but not limited to, load magnitude and direction, load duration, cyclic or static load conditions, anchor reliability, ease of installation, and anchor cost to pick the most appropriate anchoring solution.

Bonded anchors are versatile because rods/reinforcement can be cut to any length and installed with the bonding agent, and they are often faster to install than mechanical anchors. Hole cleaning and preparation are critical because anchor behavior is entirely dependent on bond at the adhesive-to-concrete interface. Mechanical anchors are often considered more reliable because they are less sensitive to hole preparation, are anchored by physical means that are less variable than bond strength, and are less susceptible to creep deformations under sustained tensile loads. The load-resisting mechanism for undercut anchors is akin to cast-in-place anchors and they are particularly reliable for resisting cyclic loads because compression/tension cycles do not degrade the anchorage. However, the installation of undercut anchors requires two drilling operations and specialized tools that increase installation time and cost. Note that mechanical anchors are only readily available in certain "off-the-shelf" lengths from manufacturers, but custom lengths may be requested from manufacturers (usually at a cost premium and with minimum quantity requirements).

EXPERIMENTAL STUDY

A set of three beams was fabricated (labeled SR1, SR2, and SR3) for the purposes of evaluating the shear strengthening techniques described in the previous section. Each beam included shear test regions at either end, resulting in six independent shear tests. Tests included one unreinforced control span, one control span reinforced with ACI 318 minimum transverse reinforcement, two spans retrofitted with undercut anchors, and two spans retrofitted with grouted anchors. Figure 5 presents an overview of the experimental program.

Specimens and test setup

The specimen dimensions, shear span-depth ratio, and longitudinal reinforcement ratio were kept constant for all tests. Each specimen was 36 in. (919 mm) wide (b) by 24 in. (610 mm) tall (h) by 332 in. (8.43 m) long. Each shear test region had an effective depth (d) of 21.3 in. (541 mm) and overall length of 53.3 in. (1353 mm), as measured between the centerlines of the applied load and the nearest support, with a resultant shear span-depth ratio (a/d) within the test region of 2.5. Specimens were reinforced with five No. 11 deformed longitudinal reinforcing bars with a resultant flexural tension reinforcement ratio of 1%.

Only the type of transverse reinforcement was varied among the six test regions. The reinforced control span used No. 4, Grade 60 deformed reinforcement in the amount required to meet ACI 318 minimum reinforcement and maximum spacing requirements (ACI 318-14 Tables 9.6.3.3 and 9.7.6.2.2). The four retrofit shear spans used Grade B7 high-strength threaded rod with 0.5 in. (12.7 mm) diameter

Table 1—Summary of material properties

Span ID	Transverse reinforcement	f_c', psi (MPa)	$f_{y,l}$, ksi (MPa)	$f_{v,v}$, ksi (MPa)	f_g', ksi (MPa)	L_a, in. (mm)
SR2S-C	None	4360 (30.1)	69.33 (478.0)	N/A	N/A	38 (965.2)
LD1N-C	None	3658 (25.2)	69.33 (478.0)	N/A	N/A	38 (965.2)
LD1S-C	None	3658 (25.2)	69.33 (478.0)	N/A	N/A	38 (965.2)
SR3N-RC	ACI minimum	3311 (22.8)	69.33 (478.0)	61.33 (422.9)	N/A	38 (965.2)
SR1S-UA	Undercut anchors	3165 (21.8)	69.33 (478.0)	118.39 (816.3)	N/A	34.75 (882.7)
SR2N-UA	Undercut anchors	4498 (31.0)	69.33 (478.0)	118.39 (816.3)	N/A	35.25 (895.4)
SR1N-GA	Grouted anchors	3304 (22.8)	69.33 (478.0)	130.37 (898.9)	8576 (59.1)	34.625 (879.5)
SR3S-GA	Grouted anchors	3190 (22.0)	69.33 (478.0)	130.37 (898.9)	9960 (68.7)	34.75 (882.7)

and 0.142 in.^{2} (91.6 mm^2) effective cross-sectional area. All transverse reinforcement (conventional and post-installed) was installed at the ACI 318 maximum allowable spacing of $d/2$ (10.5 in. [267 mm]).

Retrofit design methodology

The minimum transverse reinforcement prescribed by ACI 318 Table 9.6.3.3 served as a benchmark for development of the post-installed retrofits. ACI 318 evaluates the concrete contribution to shear strength with Eq. (22.5.5.1) (reproduced as Eq. (2) in the *Methodology for evaluation* section as follows) regardless of the amount of shear reinforcement (if any) provided. As previously noted, the Code permits some member types (for example, shallow beams, joists) to be constructed without shear reinforcement if the design shear stress does not exceed 50% of the concrete contribution to shear resistance (the limit is increased to 100% for slabs and footings).

A significant amount of research has shown that the code-prescribed value for concrete shear strength can be unconservative for large, lightly reinforced members without shear reinforcement.[15] However, tests have shown that ACI 318 conservatively estimates the concrete contribution to shear resistance for members containing at least the minimum specified amount of shear reinforcement. In most practical applications, the addition of post-installed reinforcement to an existing concrete member will provide added shear capacity owing to the steel contribution of reinforcement and potentially allow the concrete to provide sectional shear strength commensurate with Code predictions.

Selecting the ACI 318 minimum shear reinforcement for all specimens allowed researchers to directly investigate if code-prescribed spacing limitations were appropriate for post-installed retrofits, assess the repeatability of retrofit tests and what factors may impact retrofit effectiveness, and compare the load-deflection behavior of retrofit and cast-in-place options with similar amounts of reinforcement.

The relative size and spacing of the retrofit anchors (undercut and grouted) were selected to be consistent with the details developed for the control span reinforced with code-prescribed minimum transverse reinforcement. The 0.5 in. diameter undercut and grouted anchors were longitudinally spaced at $d/2$ (10.5 in. [267 mm]). An exact match between the retrofit and standard reinforcement details could not be achieved due to differences in the threaded rod cross-sectional area (29% less than the No. 4 reinforcement) and nominal yield stress (75% greater than the No. 4 reinforcement). The researchers note that ACI 318 assumes a steel contribution to shear strength proportional to its yield stress (that is, the transverse reinforcement will yield) and that the differences noted previously may have important implications. For example: 1) at the force level required to yield the No. 4 reinforcing bars, comparable retrofit anchors will elongate approximately 40% more than the standard reinforcement; and 2) the nominal yield force of the threaded rod anchors was approximately 24% greater than the nominal yield force of the deformed reinforcement.

Materials

Normalweight concrete containing 1 in. (25.4 mm) nominal crushed limestone aggregate was used for all six beams. The concrete compressive strength at the time of testing ranged from 3.1 to 4.5 ksi (21.4 to 31.0 MPa). Concrete compressive strength was determined in accordance with ASTM C39.

The measured yield strengths of the No. 11 flexural reinforcement and No. 4 transverse reinforcement were 69.3 and 61.3 ksi (478 and 423 MPa), respectively. The measured yield strengths of the undercut and grouted anchors were 118.3 and 130.3 ksi (816 and 898 MPa), respectively. Reinforcement and post-installed anchors were tested by an independent laboratory and the tensile yield strength was determined by the 0.2% offset method described in ASTM A370.

The cementitious grout used in the grouted anchor retrofits had an average compressive stress of 9.27 ksi (63.91 MPa) at the time of testing. Grout compressive strength was determined in accordance with ASTM C1019. Material properties are summarized in Table 1.

Measurements and Instrumentation

The load-deflection response of each shear test region was measured with several sensors connected to a data acquisition system. A pair of linear potentiometers at each support and the point of applied load continuously recorded displacements. A "tripod" configuration of load cells was used to continuously record load, with two of the three load cells at the support nearest the applied load and the third at the far support. Strain gauges were used to a limited extent to monitor the deformations of the cast-in-place transverse reinforcement, post-installed anchors, and longitudinal reinforcement (data not presented with this paper). Finally, crack patterns were marked between load steps, and the largest diagonal crack width was measured whenever safe.

Shear testing

Each test region was loaded monotonically in steps equivalent to approximately 10% of the nominal shear capacity estimated using the ACI 318 equations. The condition of the specimen was photographed at the end of every load step. Once load equal to roughly 80% of the nominal shear capacity had been applied, the test region was loaded continuously to failure. Testing was stopped once the load-carrying capacity fell below 70% of the peak load achieved over the course of the test. All test regions failed in shear.

The maximum applied shear (V_{ue}) and an estimate of the concrete contribution to the shear strength (V_{ce}) were recorded during each test. As defined by ACI Committee 326,[1] the experimental V_{ce} was recorded as the shear applied at the occurrence of first diagonal cracking, which was based on visual observations and was typically accompanied by a temporary reduction in applied load. The experimental steel contribution to shear capacity was further calculated as the difference between the maximum applied shear (V_{ue}) and the shear at first diagonal cracking (V_{ce}). Results will hereon be presented in terms of the normalized shear stress (v), which is defined in Eq. (1).

$$v = \frac{V}{\sqrt{f_c'} b_w d} \tag{1}$$

Test observations

Figure 6 summarizes the load-deflection response for each shear test region. The inclusion of some form of transverse reinforcement (conventional or post-installed) had a significant effect on the shear-carrying capacity of the test regions, as anticipated. Moreover, the undercut and grouted anchor retrofits performed as well as, and in some cases better than, the conventionally reinforced specimen (SR3N-RC). The normalized shear stresses resisted by the retrofitted test regions were 0.97 to 1.17 times the measured capacity of the conventionally reinforced specimen. The superior performance of the retrofitted test regions may be attributable to development of the threaded rod yield strength that was larger than the deformed reinforcement. As further noted below, the development of a single post-installed anchor was influenced by the nature of the anchorage (that is, discrete or continuous) and the location of the critical diagonal crack.

Figure 7 shows the location and orientation of diagonal cracking in each specimen. Each of the test regions with undercut anchors developed some flexure-shear cracks followed by a single, large, diagonal crack (Fig. 7(d) and (e)) like the failure crack witnessed within the unreinforced test regions (Fig. 8(a), (b) and (c)). The crack widened until force transfer was no longer possible and the test span failed. In contrast, appearance of the primary diagonal crack in test regions with grouted anchors (Fig. 7(g) and (h)) was followed by the development and growth of several smaller diagonal and flexure-shear cracks before failure of the span (indicative of force redistribution[16]). This behavior was consistent with that of the conventionally reinforced test region, and it should further be noted that the test-to-test performance was more consistent among test regions with grouted anchors.

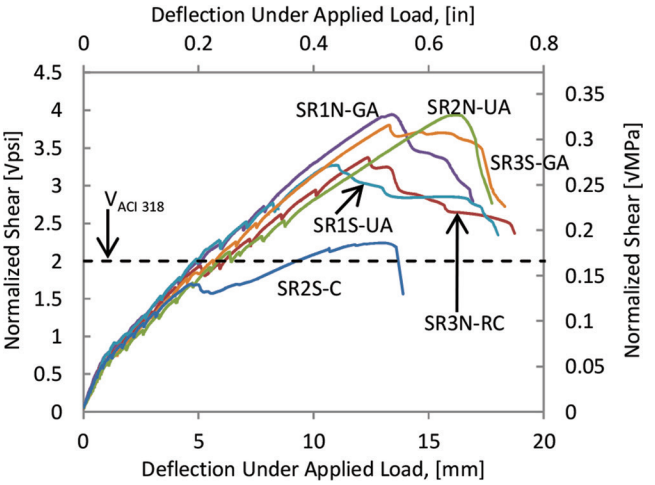

Fig. 6—Load-deflection plot for all specimens included in experimental program: (a) unreinforced control tests; and (b) transversely reinforced specimens.

In the case of the undercut anchor retrofit, the potential for force redistribution is limited because the threaded rods are mechanically anchored to the concrete at two discrete points (the anchor head and the undercut location) and as evidenced by the observed lack of secondary cracking prior to shear failure. Post-test examination of undercut anchor retrofits revealed evidence that high stresses beneath some of the washer plates caused breakout from the surrounding concrete, but it was not clear if the observed localized conditions initiated the shear failure of the specimen. This may be particularly relevant for anchors near the "tail" of the primary shear crack, where the potential breakout cone depth is limited by the proximity of the primary diagonal crack to the bottom or top face of the specimen (Fig. 8).

The continuity of bond between the threaded rod, grout, and concrete in the grouted retrofit allows internal forces to redistribute within the test region. No evidence suggesting local failures was observed and this load transfer mechanism permitted substantial, if not full, development of the threaded rod capacity. Post-test examination of grouted anchor retrofits did reveal apparent yielding of some washer plates (Fig. 8), but it was unclear whether slip of the anchor initiated the failure of the test region.

The effectiveness of post-installed reinforcement (as compared to conventional reinforcement) may be strongly influenced by the proximity of the primary shear crack to the anchorage locations of the post-installed reinforcement. In conventionally reinforced members, the yield strength of a stirrup is reliably developed due to positive anchorage around the longitudinal reinforcement (regardless of the primary shear crack position). It is not possible to anchor post-installed reinforcement in a comparable manner without additional concrete removal from the existing member. For both undercut and grouted anchors, the diagonal crack location determines the size and capacity of a potential concrete breakout cone and limits the length over which the bond between the threaded rod, grout, and concrete develops in a grouted retrofit. In members retrofitted with these techniques, the engineer is advised to consider the impact of anchor breakout/pullout in the design strength of the retrofit (Fig. 9).

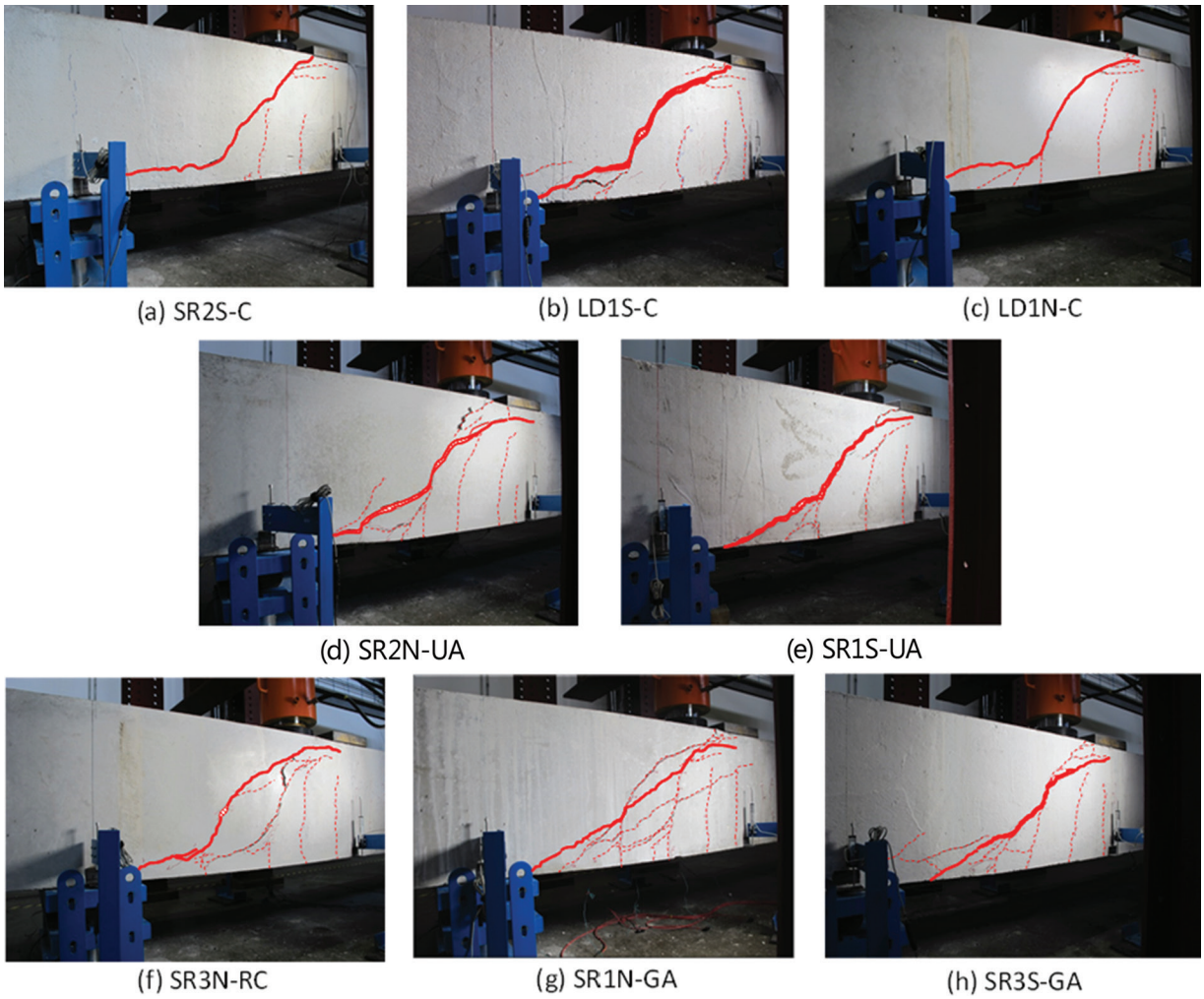

Fig. 7—Diagonal cracking pattern at failure for all specimens. Primary shear crack shown as a solid line.

METHODOLOGY FOR EVALUATION

Sectional shear strength

The experimental results of this study were compared to capacities calculated with the ACI 318-14 Building Code and the AASHTO LRFD sectional shear design provisions using measured values for material properties. The provisions were chosen as the most likely formulations to be used by engineers in the United States designing retrofits or repairs. Commonly used design specifications elsewhere—specifically CSA A23.3 and Eurocode 2—should produce estimates comparable to AASHTO LRFD, as all three specifications are based on similar simplifications to the Modified Compression Field Theory (MCFT).

ACI 318, Eq. (22.5.5.1) and (22.5.10.5.3), are reproduced as follows as Eq. (2) and (3).

$$V_c = 2\sqrt{f_c'}b_w d \tag{2}$$

$$V_s = \frac{A_v f_{y,v} d}{s} \tag{3}$$

AASHTO LRFD 2014 Eq. 5.8.3.3-3, 5.8.3.3-4, 5.8.3.4.2-2, 5.8.3.4.2-3, 5.8.3.4.2-4 (with simplifications), and 5.8.3.4.2-5 are reproduced as follows as Eq. (4) through (9).

$$V_c = 0.0316\beta\sqrt{f_c'}b_v d_v \tag{4}$$

$$V_s = \frac{A_v f_y d_v \cot(\theta)}{s} \tag{5}$$

$$\beta = \frac{4.8}{(1+750\varepsilon_s)}\frac{51}{(39+s_{xe})} \tag{6}$$

$$\theta = 29 + 3500\varepsilon_s \tag{7}$$

$$\varepsilon_s = \frac{\left(\frac{|M_u|}{d_v} + |V_u|\right)}{E_s A_s} \tag{8}$$

$$s_{xe} = s_x \frac{1.38}{a_g + 0.63} \tag{9}$$

Post-installed reinforcement strength

As noted previously, anchorage and bond conditions may impact the effectiveness of post-installed reinforcement in shear retrofit applications, especially when the geometry of the primary shear crack reduces the effective embedment of

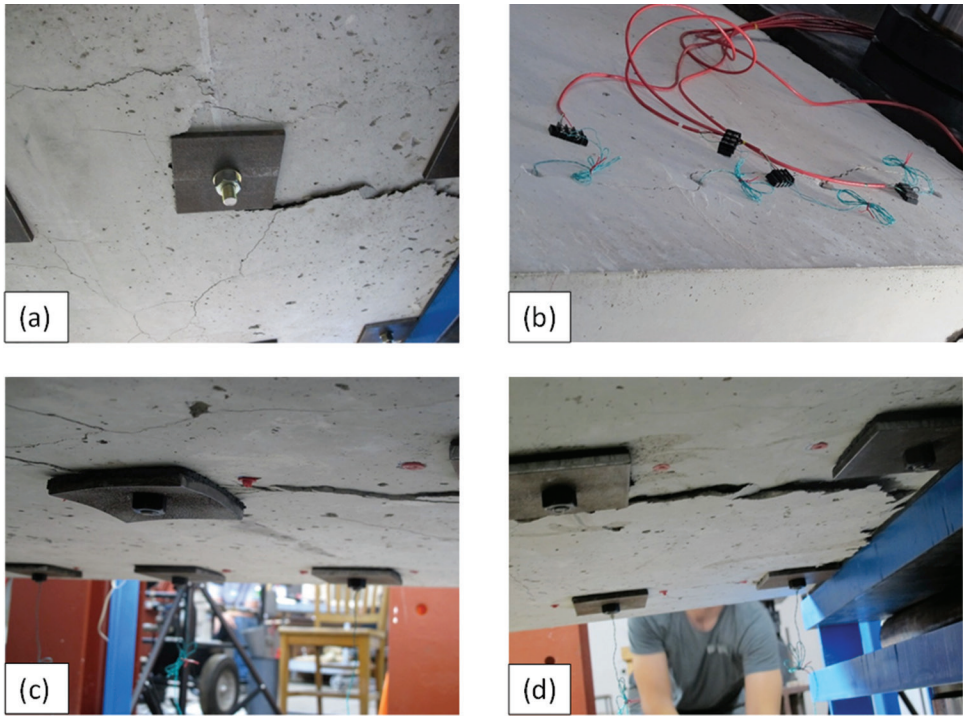

Fig. 8—Localized distress near anchor reinforcement: (a) undercut anchor plate "punching through" tension face of beam; (b) splitting between undercut anchor locations; (c) washer plate yielding; and (d) structural core concrete failing between regions confined by post-installed anchors.

a post-installed anchor. ACI 318, Chapter 17, "Anchoring to Concrete," is used as the basis for evaluating the impact of concrete breakout and grout-concrete bond failure on development of the full strength of post-installed reinforcement. The Chapter 17 provisions consider the following failure mechanisms (relevant to this study) for anchors subjected to tension: steel fracture; concrete breakout; anchor pullout; and anchor bond strength. ACI 318, Eq. (17.4.1.2) (steel fracture), (17.4.2.1b) (concrete breakout, mechanical anchor), (17.4.3.4) (headed bolt pullout), and (17.4.5.1b) (concrete breakout, adhesive anchor) are reproduced below as Eq. (10) through (13). Reference ACI 318-14, Chapter 17, for more detailed information and notation.

$$N_{sa} = A_{se,N} f_{uta} \tag{10}$$

$$N_{cbg} = \frac{A_{Nc}}{A_{Nco}} \psi_{ec,N} \psi_{ed,N} \psi_{c,N} \psi_{cp,N} N_b \tag{11}$$

$$N_p = 8 A_{brg} f_c' \tag{12}$$

$$N_{ag} = \frac{A_{Na}}{A_{Nao}} \psi_{ec,Na} \psi_{ed,Na} \psi_{cp,Na} N_{ba} \tag{13}$$

For the purposes of this study, each pair of post-installed anchors acting as a stirrup was treated as a two-anchor group whose strength was evaluated in accordance with the provisions of ACI 318, Chapter 17. Two pairs of anchors were considered to contribute to the sectional shear strength of the test region, and the capacity of each anchor pair was

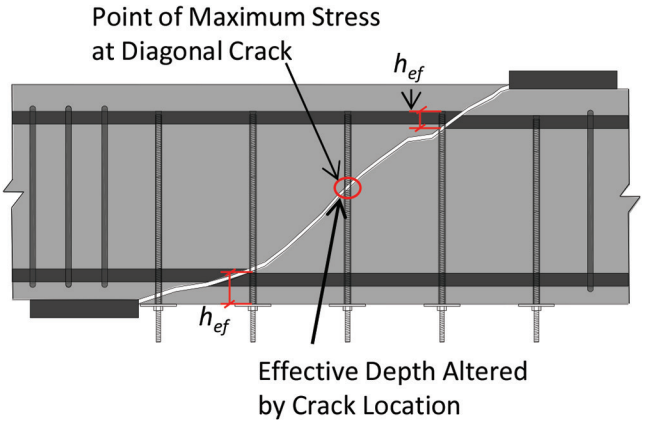

Fig. 9—Impact of diagonal crack location on effective embedment depths of post-installed reinforcement. Only the test region of specimen is shown.

calculated using an "average" effective depth equal to the distance between the point of anchorage and the primary shear crack, assuming the primary shear crack formed near midheight of the anchors. The controlling limit state among concrete breakout, anchor pullout, bond failure, and steel yield was used as the calculated V_{sn}. This approach is similar to the modified truss analogy that forms the basis of Eq. (3) (ACI 318, Eq. (22.5.10.5.3)) and does not explicitly account for the variable effective embedment depth of different anchors based on the orientation of the primary shear crack. Chapter 17 does not include grout-in-place anchors within its scope but the researchers feel that Eq. (12) is nonetheless an appropriate estimation of the bond strength at the grout-concrete interface.[13,14]

Calculation of nominal capacity for comparison to experimental results

Using the information presented previously, four independent nominal capacities were calculated for comparison to the experimental results. In subsequent sections of this paper, the calculation methods are referred to as "ACI 318", "ACI 318-Mod", "AASHTO", and "AASHTO-Mod". The combinations of equations used to calculate nominal capacities for each method are summarized as follows:

1. "ACI 318"—V_{cn} and V_{sn} calculated by Eq. (1) and (2), respectively;
2. "ACI 318-Mod"—V_{cn} calculated by Eq. (1) and V_{sn} calculated as the minimum of Eq. (10) through (13);
3. "AASHTO"—V_{cn} and V_{sn} calculated by application of Eq. (4) through (9); and
4. "AASHTO-Mod"—V_{cn} and V_{sn} calculated by application of Eq. (4) through (9), except that f_y is modified such that the total tension force provided by one post-installed anchor is equal to the value calculated by ACI 318, Chapter 17, as determined previously.

ANALYSIS OF RESULTS

Figure 10 and Table 2 present a concise comparison between experimental results and calculated capacities as

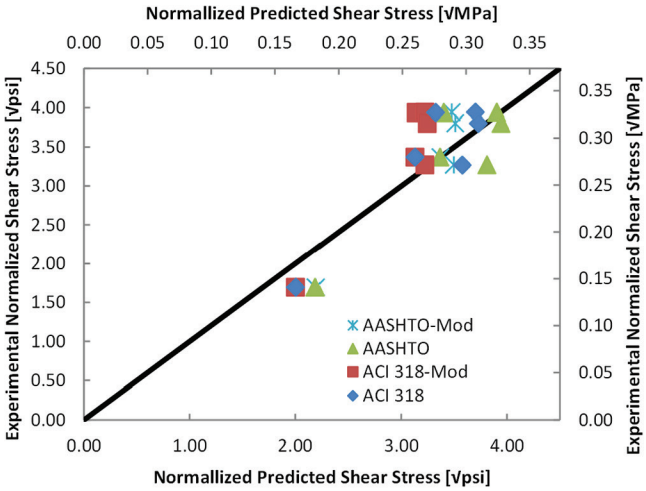

Fig. 10—Comparison of experimental results and code predictions using actual material properties.

Table 2—Summary of experimental test results and comparison to analytical predictions

	Span ID	V_e, lb (kN)	V_{ACI}, lb (kN)	V_e/V_{ACI}	$V_{ACI\text{-}Mod}$, lb (kN)	$V_e/V_{ACI\text{-}Mod}$	V_{AASHTO}, lb (kN)	V_{test}/V_{AASHTO}	$V_{AASHTO\text{-}Mod}$, lb (kN)	$V_e/V_{AASHTO\text{-}Mod}$
Concrete contribution V_c	SR2S-C	85,905 (382.3)	101,240 (450.5)	0.85	101,240 (450.5)	0.85	110,659 (492.4)	0.78	110,659 (492.4)	0.78
	SR3N-RC	85,161 (379.0)	88,225 (392.6)	0.97	88,225 (392.6)	0.97	83,139 (370.0)	1.02	83,139 (370.0)	1.02
	SR1S-UA	93,013 (413.9)	86,258 (383.8)	1.08	86,258 (383.8)	1.08	76,853 (342.0)	1.21	80,567 (358.5)	1.15
	SR2N-UA	109,048 (485.3)	102,830 (457.6)	1.06	102,830 (457.6)	1.06	88,450 (393.6)	1.23	90,862 (404.3)	1.20
	SR1N-GA	94,947 (422.5)	88,131 (392.2)	1.08	88,131 (392.2)	1.08	76,528 (340.5)	1.24	81,681 (363.5)	1.16
	SR3S-GA	79,850 (355.3)	86,598 (385.4)	0.92	86,598 (385.4)	0.92	75,440 (335.7)	1.06	80,556 (358.5)	0.99
Steel contribution V_s	SR3N-RC	63,531 (282.7)	49,729 (221.3)	1.28	49,729 (221.3)	1.28	65,246 (290.3)	0.97	65,246 (290.3)	0.97
	SR1S-UA	48,060 (213.9)	68,138 (303.2)	0.71	52,835 (235.1)	0.91	87,314 (388.5)	0.55	70,257 (312.6)	0.68
	SR2N-UA	93,415 (415.7)	68,138 (303.2)	1.37	58,496 (260.3)	1.60	86,083 (383.1)	1.09	75,713 (336.9)	1.23
	SR1N-GA	78,838 (350.8)	75,050 (334.0)	1.05	53,983 (240.2)	1.46	95,182 (423.6)	0.83	71,294 (317.3)	1.11
	SR3S-GA	84,803 (377.4)	75,050 (334.0)	1.13	53983 (240.2)	1.57	95,307 (424.1)	0.89	71,395 (317.7)	1.19
Total shear strength V_n	SR2S-C	85,905 (382.3)	101,240 (450.5)	0.85	101,240 (450.5)	0.85	110,659 (492.4)	0.78	110,659 (492.4)	0.78
	SR3N-RC	148,692 (661.7)	137,954 (613.9)	1.08	137,954 (613.9)	1.08	148,384 (660.3)	1.00	148,384 (660.3)	1.00
	SR1S-UA	141,073 (627.8)	154,396 (687.1)	0.91	139,092 (619.0)	1.01	164,167 (730.5)	0.86	150,824 (671.2)	0.94
	SR2N-UA	202,463 (901.0)	170,968 (760.8)	1.18	161,326 (717.9)	1.25	174,534 (776.7)	1.16	166,575 (741.3)	1.22
	SR1N-GA	173,785 (773.3)	163,181 (726.2)	1.06	142,114 (632.4)	1.22	171,710 (764.1)	1.01	152,975 (680.7)	1.14
	SR3S-GA	164,653 (732.7)	161,648 (719.3)	1.02	140,580 (625.6)	1.17	170,748 (759.8)	0.96	151,951 (676.2)	1.08

Table 3—Comparison of capacity calculation methods

Calculation method	Specimen	$V_{n,test}$, √psi (√MPa)	$V_{n,calc}$, √psi (√MPa)	$V_{n,test}/V_{n,calc}$	Average	Coefficient of variation
ACI 318	SR3-N	3.37 (0.28)	3.13 (0.26)	1.08	1.05	0.09
	SR2-N	3.94 (0.33)	3.33 (0.28)	1.18		
	SR1-N	3.94 (0.33)	3.70 (0.31)	1.06		
	SR1-S	3.27 (0.27)	3.58 (0.30)	0.91		
	SR3-3	3.80 (0.32)	3.73 (0.31)	1.02		
ACI 318-MOD	SR3-N	3.37 (0.28)	3.13 (0.26)	1.08	1.15	0.09
	SR2-N	3.94 (0.33)	3.14 (0.26)	1.25		
	SR1-N	3.94 (0.33)	3.23 (0.27)	1.22		
	SR1-S	3.27 (0.27)	3.23 (0.27)	1.01		
	SR3-3	3.80 (0.32)	3.25 (0.27)	1.17		
AASHTO	SR3-N	3.37 (0.28)	3.36 (0.28)	1.00	1.00	0.11
	SR2-N	3.94 (0.33)	3.39 (0.28)	1.16		
	SR1-N	3.94 (0.33)	3.90 (0.32)	1.01		
	SR1-S	3.27 (0.27)	3.81 (0.32)	0.86		
	SR3-3	3.80 (0.32)	3.94 (0.33)	0.96		
AASHTO-MOD	SR3-N	3.37 (0.28)	3.36 (0.28)	1.00	1.07	0.10
	SR2-N	3.94 (0.33)	3.24 (0.27)	1.22		
	SR1-N	3.94 (0.33)	3.47 (0.29)	1.14		
	SR1-S	3.27 (0.27)	3.50 (0.29)	0.94		
	SR3-3	3.80 (0.32)	3.51 (0.29)	1.08		

described in the previous section. Recall that the experimental concrete contribution V_{ce} was estimated as the load to produce first visible diagonal cracking; the experimental steel contribution V_{se} is a quantity back-calculated by subtracting V_{ce} from the peak test load V_{ue}. In addition, the critical section for shear was assumed to be the middle of the shear span (that is, $a/2$ = 26.6 in. [676 mm] from the center of the applied load). Table 3 compares total nominal calculated shear capacity to experimental shear capacity for test specimens with reinforcement only, including the mean and coefficient of variation, and demonstrates good agreement between calculated and experimental capacities.

The ACI 318 and AASHTO LRFD provisions, without modifications, offered similar levels of accuracy and closely approximated the experimental shear strength of test specimens. Analysis of experimental results indicates that ACI 318 and AASHTO provisions modified by provisions of ACI 318 Chapter 17 indicates that this approach is conservative because the experimental capacity consistently exceeded the calculated capacity (except for specimen SR1-S).

While concrete breakout or bond slip may not have initiated shear failure of the test specimens, researchers observed signs of anchorage distress during post-test examination. Further, ACI 318 and AASHTO LRFD provisions modified to account for anchor limit states conservatively predict total sectional shear strength. Designers should carefully consider concrete breakout, bond, and other local limit states when designing post-installed shear reinforcement for flexural members.

CONCLUSIONS

Based on the experimental program described herein and the comparison of experimental and calculated capacities, the researchers conclude that:

1. Strength and deformation capacity of members without transverse reinforcement is increased significantly with post-installed transverse reinforcement. Behavior under static loading conditions is similar to that of specimens containing cast-in-place transverse reinforcement; this is especially true for grouted anchors, which have a continuous bond along the length of the anchors.

2. Consideration of alternate modes of anchor failure (that is, failure prior to yielding), including concrete breakout, bond failure, and local anchorage failure, is necessary to obtain a reasonable strength estimate. Further research should be conducted to better characterize how non-yielding reinforcement failure modes affect the shear strength provided by post-installed reinforcement.

3. Both the retrofit techniques studied herein only require access to one side of a structural member and are therefore ideal for situations with limited access or where limited disruption is desirable. Of the two studied techniques, undercut anchors may be considerably easier to install in horizontal or overhead applications.

4. Calculations presented herein use actual material properties and do not make use of load, resistance, or safety factors. Consideration of nominal material properties and load and resistance or safety factors will add appropriate safety margins to the design. The authors recommend further research be conducted to assign statistically appropriate

shear resistance factors to structural elements with post-installed reinforcement.

AUTHOR BIOS

Anthony Dondrea *is a Structural Engineer at Simpson Gumpertz and Heger, Inc., Washington, DC. He received his Bachelor of Science degree in architectural engineering in 2012 and his Master of Science degree in civil engineering in 2014 from the University of Texas at Austin, Austin, TX. He worked in the Ferguson Structural Engineering Laboratory during his graduate studies. His research interests include design, investigation, and rehabilitation of structures with a focus on concrete repair.*

Oguzhan Bayrak, *FACI, is a University Distinguished Teaching Professor and holds the Charles Elmer Rowe Fellowship at the University of Texas at Austin. He is a member of ACI Committee 341, Earthquake-Resistant Concrete Bridges, and Joint ACI-ASCE Committees 441, Reinforced Concrete Columns, and 445, Shear and Torsion.*

ACKNOWLEDGMENTS

The research described in this paper was funded by MPR Associates and their support in this effort, as well as others at the University of Texas, is greatly appreciated. Support from many graduate students at the University of Texas made this project possible: N. Dassow, G. Arietta-Martinez, D. Wald, J. Klein, S. Watts, and others. Special thanks to D. Deschenes for his invaluable contributions to developing the research program and technical guidance.

NOTATION

A_s = total area of longitudinal tension reinforcement
A_v = effective area of transverse reinforcement within spacing, s
a = shear span; distance between centerline of applied load and nearest support
a_g = maximum diameter of aggregate
b_v = AASHTO section width effective in resisting shear
b_w = width of web; equivalent to section width for rectangular geometries
d = effective depth of tension reinforcement; distance from compression face to centroid of longitudinal tension reinforcement
d_v = AASHTO effective shear depth
f_c' = concrete compressive strength
f_y = yield strength of longitudinal tension reinforcement
$f_{y,v}$ = yield strength of transverse reinforcement
h_{ef} = effective anchor embedment depth
M_u = moment at critical section for shear—that is, moment at a/2
s = center-to-center spacing of transverse reinforcement
s_x = factor used to calculate crack spacing parameter s_{xe}, as defined by AASHTO
s_{xe} = crack spacing parameter as defined by AASHTO
V = shear force
V_{AASHTO} = calculated sectional shear at critical section, using unmodified provisions of AASHTO-LRFD
$V_{AASHTO\text{-}mod}$ = calculated sectional shear at critical section, using modified provisions of AASHTO-LRFD
V_{ACI} = calculated sectional shear at critical section, using unmodified provisions of ACI 318-14
$V_{ACI\text{-}mod}$ = calculated sectional shear at critical section, using modified provisions of ACI 318-14
V_c = concrete contribution to shear resistance
V_{ce} = experimental concrete contribution to shear resistance
V_{cn} = calculated concrete contribution to shear resistance
V_s = steel contribution to shear resistance
V_{se} = experimental steel contribution to shear resistance
V_{sn} = calculated steel contribution to shear resistance
V_u = sectional shear at critical section—that is, shear at a/2
V_{ue} = experimental sectional shear at critical section—that is, shear at a/2
V_{un} = calculated sectional shear at critical section—that is, shear at a/2
α = relative angle between beam longitudinal axis and axis of transverse reinforcement
β = factor accounting for cracked concrete's ability to transfer tension/shear as defined by AASHTO-LRFD
ε_s = longitudinal tensile strain at centroid of tension reinforcement
θ = angle of inclination of diagonal compressive stresses
ν = normalized shear stress
ρ_w = longitudinal reinforcement ratio

REFERENCES

1. Joint ACI-ASCE Committee 326, "Shear and Diagonal Tension," *ACI Journal Proceedings*, V. 59, No. 1-3, Jan.-Mar., 1962, pp. 1-30, 277-344, and 352-396.

2. ACI Committee 364, "Increasing Shear Capacity within Existing Reinforced Concrete Structures (ACI 364.2T-08)," American Concrete Institute, Farmington Hills, MI, 2008, 4 pp.

3. Kunz, J., and Randl, N., "Strengthening and Design of Shear Beams," *Tailor Made Concrete Structures*, J. C. Walraven and D. Stoelhorst, eds., 2008, pp. 657-663.

4. Kunz, J., "Strengthening with Post-installed Shear Reinforcement," *Conservation of Structures*, 2013, pp. 154-158.

5. Ruiz, M. F.; Muttoni, A.; and Kunz, J., "Strengthening of Flat Slabs against Punching Shear Using Post-Installed Shear Reinforcement," *ACI Structural Journal*, V. 107, No. 4, July-Aug. 2010, pp. 434-442.

6. Heymsfield, E., and Durham, S. A., "Retrofitting Short-Span Precast Channel Beam Bridges Constructed without Shear Reinforcement," *Journal of Bridge Engineering*, ASCE, V. 16, No. 3, 2011, pp. 445-452. doi: 10.1061/(ASCE)BE.1943-5592.0000167

7. Barros, J. A. O., and Dalfré, G. M., "Assessment of the Effectiveness of the Embedded Through-Section Technique for the Shear Strengthening of Reinforced Concrete Beams," *Strain*, V. 49, No. 1, 2013, pp. 75-93. doi: 10.1111/str.12016

8. Chaallal, O.; Mofidi, A.; Benmokrane, B.; and Neale, K., "Embedded Through-Section FRP Rod Method for Shear Strengthening of RC Beams: Performance and Comparison with Existing Techniques," *Journal of Composites for Construction*, ASCE, V. 15, No. 3, 2011, pp. 374-383. doi: 10.1061/(ASCE)CC.1943-5614.0000174

9. Randl, N., "Research on Post-Installed Reinforcement for Structural Retrofitting," *Proceedings of 18th Congress of IABSE*, Seoul, South Korea, 2012, 5 pp.

10. ACI Committee 318, "Building Code Requirements for Structural Concrete (ACI 318-14) and Commentary (ACI 318R-14)," American Concrete Institute, Farmington Hills, MI, 2014, 520 pp.

11. *AASHTO LRFD Bridge Design Specifications*, seventh edition, American Association of State and Highway Transportation Officials, Washington, DC, 2014.

12. Bissonnette, B.; Vaysburd, A. M.; and Von Fay, K. F., "Best Practices for Preparing Concrete Surfaces Prior to Repairs and Overlays," *Report* No. MERL 12-17, U.S. Department of the Interior, Bureau of Reclamation, Denver, CO, 2012.

13. Cook, R. A.; Collins, D. M.; Klingner, R. E.; and Polyzois, D., "Load-Deflection Behavior of Cast-in-Place and Retrofit Concrete Anchors," *ACI Structural Journal*, V. 89, No. 6, Nov.-Dec. 1992, pp. 639-649.

14. Zamora, N. A.; Cook, R. A.; Konz, R. C.; and Consolazio, G. R., "Behavior and Design of Single, Headed and Unheaded, Grouted Anchors under Tensile Load," *ACI Structural Journal*, V. 100, No. 2, Mar.-Apr. 2003, pp. 222-230.

15. Collins, M. P., and Kuchma, D., "How Safe Are Our Large, Lightly Reinforced Concrete Beams, Slabs, and Footings?" *ACI Structural Journal*, V. 96, No. 4, July-Aug. 1999, pp. 482-491.

16. Wight, J. K., and MacGregor, J. G., *Reinforced Concrete Mechanics and Design*, sixth edition, Pearson, Boston, MA, 2012.